Hypernuclei Studies:
A Key to Resolving the Hyperon Puzzle in NSs

LI Ang 李昂
liang@xmu.edu.cn
Xiamen U.

Based on arXiv: 2205.10631 ApJ
and ongoing works with
Shiyuan Ding, Baoyuan Sun (LZU, Lanzhou)
Jinniu Hu, Hong Shen (NKU, Tianjin)

Many thanks for Invitation!

Nucleosynthesis and Evolution of Neutron Stars
27-30 Jan 2025 Kyoto University, Japan

Why is understanding the EoS important for nuclear/astrophysicists?

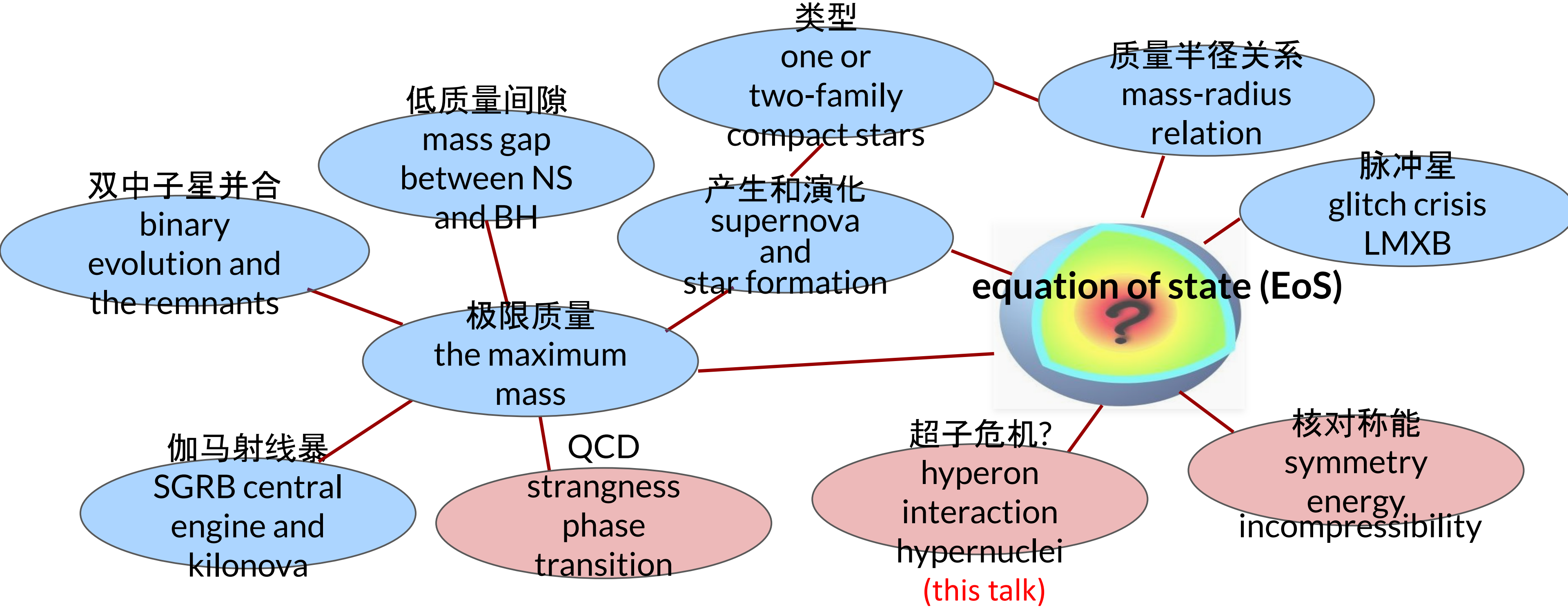

The Astrophysical Journal, 942:55 (13pp), 2023 January 1 https://doi.org/10.3847/1538-4357/ac9d9a

OPEN ACCESS

2205.10631

Astrophysical Implications on Hyperon Couplings and Hyperon Star Properties with Relativistic Equations of States

Xiangdong Sun[1], Zhiqiang Miao[1], Baoyuan Sun[2], and Ang Li[1]
[1] Department of Astronomy, Xiamen University, Xiamen, Fujian 361005, People's Republic of China; liang@xmu.edu.cn
[2] Frontiers Science Center for Rare Isotopes, Lanzhou University, Lanzhou 730000, People's Republic of China

From Referee "The present article addresses a long-standing issue in neutron star physics, namely the hyperon puzzle. The authors incorporate new information from hypernuclei calculations and **treat the hyperon couplings in a more general way** than what exists in the present literature. This is an interesting work that can have important future implications."

an RMF with density dependent couplings. The authors of Sun et al. (2023) have recently developed a Bayesian inference approach, in the framework of several nuclear RMF, to determine how GW and NICER measurements constrain the $\Lambda-\sigma$ and $\Lambda-\omega$ couplings, while fixing the Σ and Ξ couplings to reasonable values. A major advantage of this methodology is the possibility, once the inference is completed, to discuss the possible composition of matter or the nuclear properties. In the present study, we will base our approach

A **major advantage** of this methodology is the possibility, once the inference is completed, to discuss the possible composition of matter or the nuclear properties.

Huang, Raaijmakers, Watts, Tolos, & Providência, 2303.17518 MNRAS

Outline

- **Basic** for neutron star structure and the EoS
- **Recent work** on connecting #consistently NS observations and (hyper)nuclear experiments
- **Summary and Exciting future**

What is the nature of the particles that make up neutron stars?

Lev Landau

James Chadwick

Walter Baade

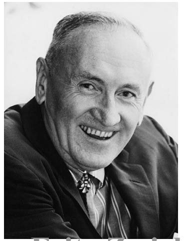

Fritz Zwicky

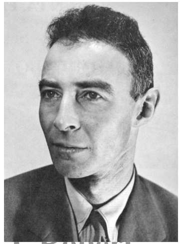

J. Robert Oppenheimer

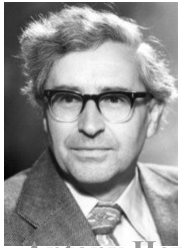

Antony Hewish

Nobel prize 1974

Dame Jocelyn Bell Burnell

1967

Fundamental Physics Breakthrough Prize 2018

1932-

“the density of matter becomes so great that atomic nuclei come in close contact, forming one ***gigantic nucleus****.”*

A ~ 10^{57}; For R=10 km, M=1.4 $M_\odot$, average density ~(2-3) nuclear density ϱ_0

~several hundreds MeV (nonperturbative)

Extreme conditions make it impossible to attain by theo./exp. methods only.

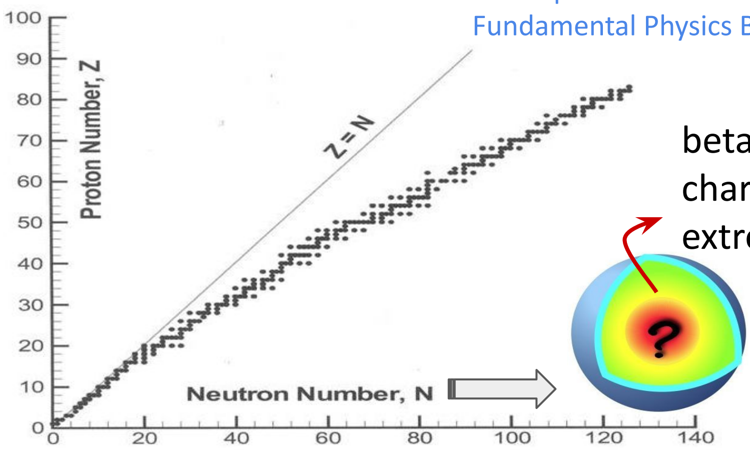

beta equilibrium;
charge neutrality;
extremely neutron-rich

EoS uncertainty from QCD **phase uncertainty** and **model uncertainty**

- Hyperon **puzzle**; Δ(1232)/hyperon/Kaon/quark **complication**
- 1) Unified crust-core; 2) High-density extrapolation

Hyperon puzzle: Heavy pulsars larger than $2M_\odot$ is a pain

BHF (NN + NNN + NY)

fitted from scattering data

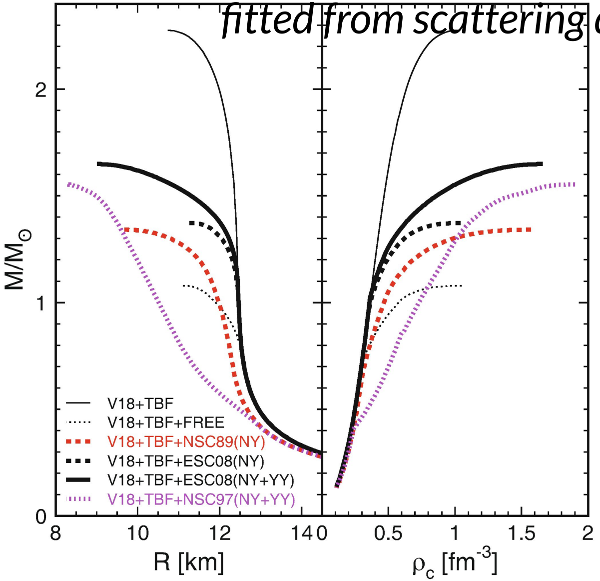

Schulze & Rijken 2016

RMF(NN+NY+YY)

consistent with hypernuclei data

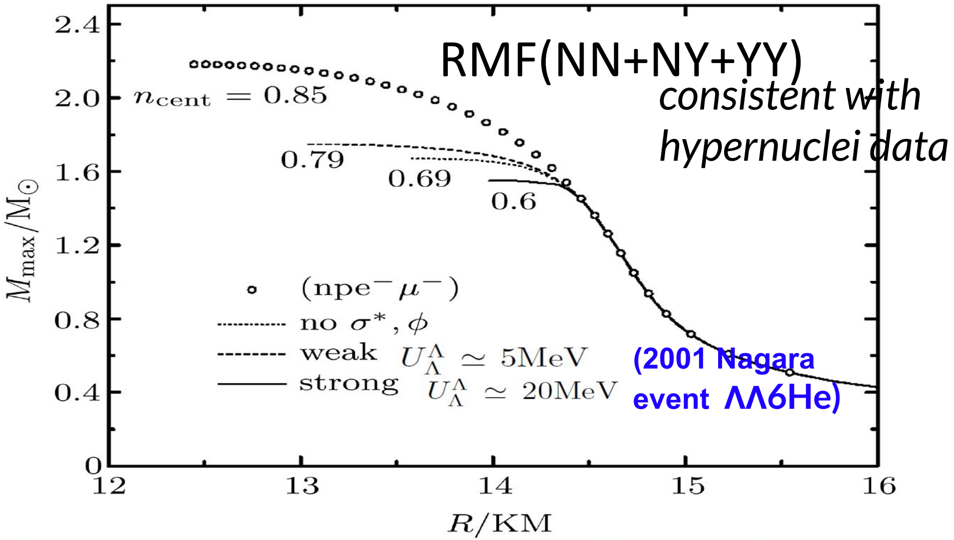

Fig.3. The mass–radius relation calculated for the strong and weak hyperon–hyperon interaction models, in comparison with the one without strange mesons ($\sigma*, \phi$), and also the results without hyperons. See text for details.

Li et al. 2007

Is it possible to combine NS multi-messenger (2017-) observations with hypernuclei experiments to understand better the hypernuclear force? **How**? **What new**?

Neutron star group @XMU

arXiv:2412.09219 Submitted
arXiv:2408.15022 MNRAS
arXiv:2402.02799 PRD
arXiv:2312.17102 ApJ
arXiv:2312.12185 ApJ
arXiv:2312.04305 MNRAS
arXiv:2305.16058 PRC
arXiv:2305.08401 ApJ
arXiv:2304.12050 PRD
arXiv:2211.04978 PRD
arXiv:2211.02007 ApJ
arXiv:2205.10631 ApJ
arXiv:2204.05560 ApJ
arXiv:2203.04798 PRD
arXiv:2201.12053 PRC
arXiv:2108.00560 ApJ
arXiv:2107.13997 ApJL
arXiv:2107.07979 MNRAS
arXiv:2103.15119 ApJ
arXiv:2011.11934 ApJ
arXiv:2009.12571 MNRAS
arXiv:2007.05116 JHEAp (review)
arXiv:2006.00839 ApJ
arXiv:2005.12875 ApJS
arXiv:2005.02677 PRD
arXiv:2001.03859 PRC

Zhenyu Zhu 朱镇宇

Many-body theory;
Merger simulation
Numerical relativity

Graduated in 2021; postdoc in CCRG-RIT

Zhiqiang Miao 缪志强

Hybrid star;
Quark matter;
Bayesian analysis
GR

Graduated in 2023; postdoc in TDLee inst.

Zhonghao Tu 涂中豪

Superfluidity;
Neutron star cooling;
Nuclear pinning force

Wenli Yuan 苑文莉

Quark matter;
QCD phase diagram

Graduated in 2023; postdoc in PKU

Peng Liu 刘鹏

Glitch;
Pulsar observation

Xiangdong Sun 孙向东

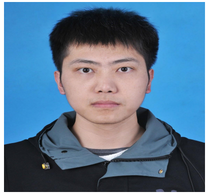

Nuclear matter;
Hyperon matter;
Many-body theory

Shuochong iHan 韩烁冲

Many-body theory;
Nuclear transport

with 4 undergraduate students

Outline

- **Basic** for neutron star structure and the EOS
- **Recent work** towards the determination of the #(hyper)nuclear force and NS properties from multimessenger astronomy
  (Biased selected results; Highlighing work done by our group)
- **Summary and Exciting future**

Black box = EoS microphysics

Procedure used until now

$$\Gamma = (\rho + P)(dP/d\rho)/P$$

- ❑ Piecewise polytrope EoS: Logarithm of the adiabatic index (Γ) of the EoSs are treated as polynomial: **Little to no microphysics;**

Better procedure

- ❑ More physics at the EoS modelling stage;
- ❑ Support **quantitative** studies of the EoS at different density regimes;
- ❑ With prior **explicitly** considering phase transition;
- ❑ Can discuss the **composition** of matter and the underlying strong **interaction**;
- ❑ Allow for straightforward **extensions** to higher-dimensional models, accommodating the inclusion of additional particles within NSs, even dark matter;
- ❑ Facilitate a **connection** with the ongoing research efforts in the field of relativistic HIC.

EoS: The roadmap

1. Model for interaction between particles

$$\hat{\mathcal{H}}\Psi = E\Psi$$

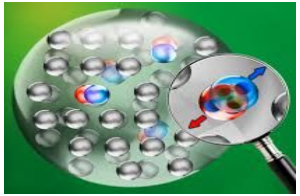

2. EoS prior pasting test

$$G_{\mu\nu} = \frac{8\pi G}{c^4} T_{\mu\nu}$$

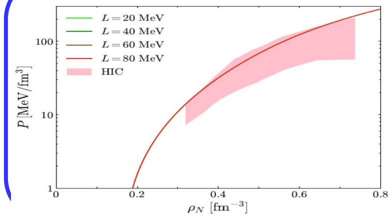

3. EoS inference from NS obs. (GW, photons, neutrinos)

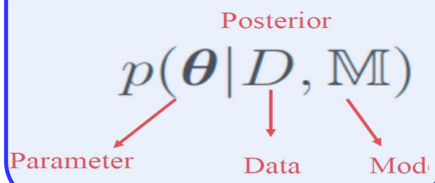

Physics on the EoS, the composition and the underlying strong interaction

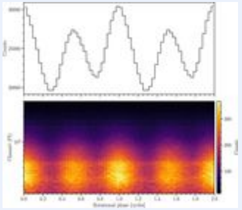

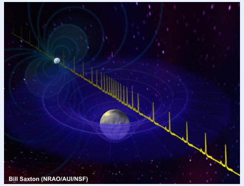

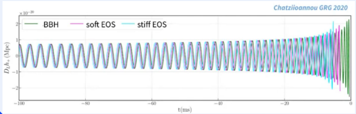

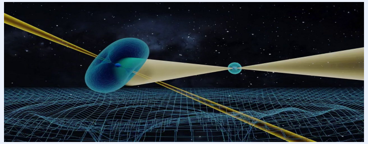

Prepare EoS prior starting for e.g., RMF parameter set

1. Model for interaction between particles → **2. the EoS** → **3. NS observations (M-R relation, Lambda)**

$$\hat{\mathcal{H}}\Psi = E\Psi \qquad\qquad G_{\mu\nu} = \frac{8\pi G}{c^4}T_{\mu\nu}$$

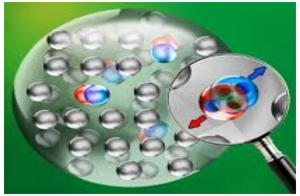

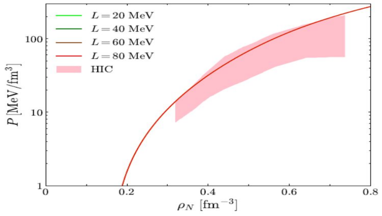

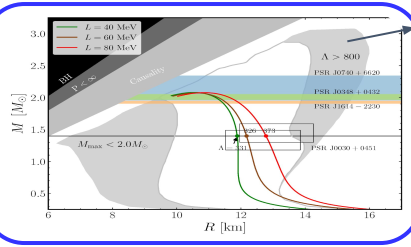

excluded by $\Lambda(1.4) \lesssim 800$ of GW170817

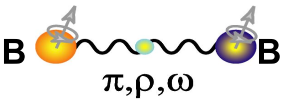

(P, I, J symmetry)

$$\mathcal{L} = \overline{\psi}\left(i\gamma_\mu\partial^\mu - M_N^* - g_{\omega N}\omega\gamma^0 - g_{\rho N}\rho\tau_3\gamma^0\right)\psi - \frac{1}{2}(\nabla\sigma)^2 - \frac{1}{2}m_\sigma^2\sigma^2 - \frac{1}{3}g_2\sigma^3 - \frac{1}{4}g_3\sigma^4$$
$$+\frac{1}{2}(\nabla\rho)^2 + \frac{1}{2}m_\rho^2\rho^2 + \frac{1}{2}(\nabla\omega)^2 + \frac{1}{2}m_\omega^2\omega^2 + \frac{1}{2}g_{\rho N}{}^2\rho^2\Lambda_v g_{\omega N}{}^2\omega^2,$$

Static approximation considered in the Lagrangian on mesons so that their time components are neglected;

Spatial part of **ω** meson disappears for the time reversal symmetry;

Infinite nuclear matter has translational invariance, removing the partial part of the coordinate space.

Eqs. of motion of baryons and mesons can be generated by the Euler-Lagrangian eq. from the Lagrangian:

$$\left[i\gamma^\mu\partial_\mu - M_B^* - \gamma^0\left(g_{\omega B}\omega + g_{\phi B}\phi + \frac{g_{\rho B}}{2}\rho\tau_3\right)\right]\psi_B = 0,$$
$$m_\sigma^2\sigma + g_2\sigma^2 + g_3\sigma^3 = \sum_B g_{\sigma B}\rho_B^s,$$
$$m_\omega^2\omega + c_3\omega^3 + 2\Lambda_v\left(g_{\omega N}^2\omega\right)\left(g_{\rho N}^2\rho^2\right) = \sum_B g_{\omega B}\rho_B^v,$$
$$m_\rho^2\rho + 2\Lambda_v(g_{\omega N}^2\omega^2)(g_{\rho N}^2\rho) = \sum_B \frac{g_{\rho B}}{2}\rho_B^{v3},$$

Then, p & ε (with arbitrary isospin asymmetry) from nuclear part can be generated by the energy-momentum tensor.

Employed 18 stiff relativistic EoSs with 7 types of variation of the RMF effective interactions

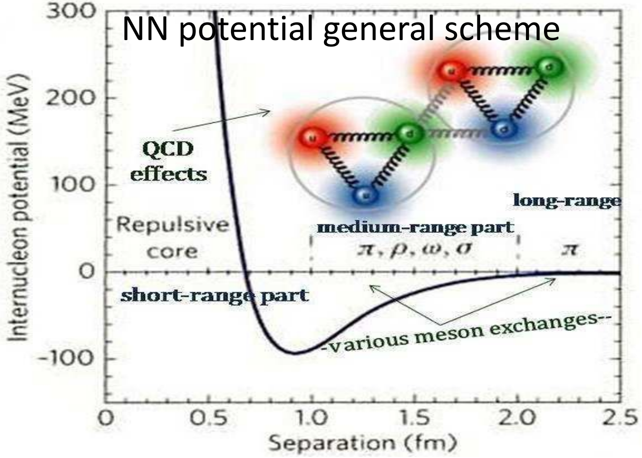

1) Original linear Walecka model,
2) Nonlinear Walecka model with σ **self-interacting** mesons
3) Nonlinear Walecka model with σ, ω **self-interacting** mesons,
4) Nonlinear Walecka model with σ, ω **self-interacting** mesons and possible mesonic **cross** terms,
5) Models in which the parameters that couple the baryons with the mesons are **density-dependent**,
6) Models with the inclusion of $\boldsymbol{\delta}$ mesons, i.e., $a_0(980)$,
7) **Point-coupling (PC)** models without exchanging mesons.

Reproducing nuclear saturation with varying stiffness

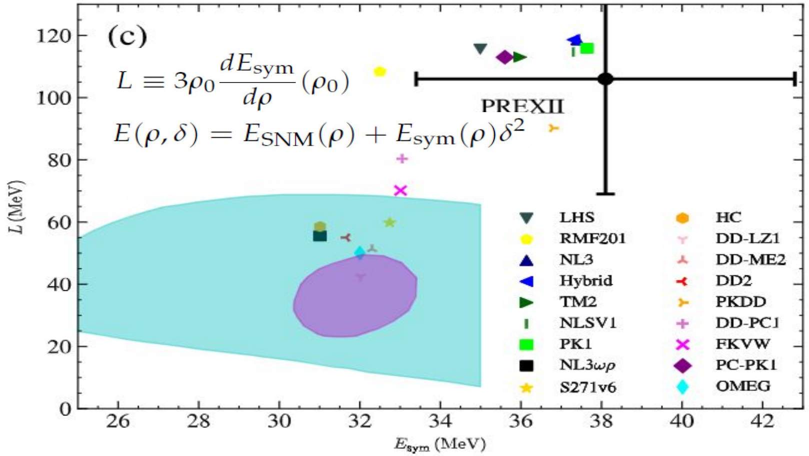

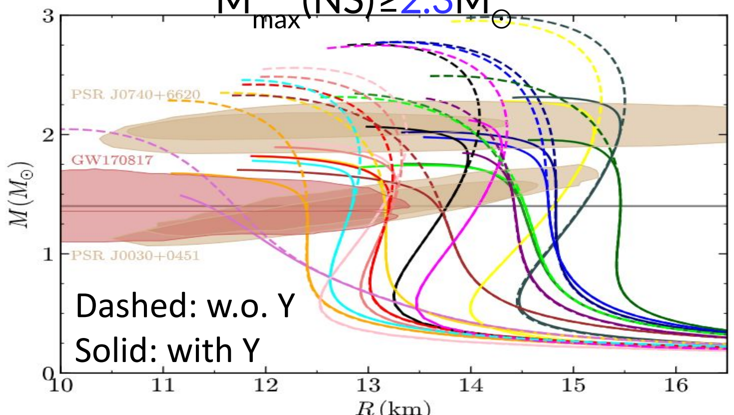

To combine (binary) NS observations with hypernuclei experiments

$$p(\boldsymbol{\theta}, D) \propto \pi(\boldsymbol{\theta}) \times L(D|\boldsymbol{\theta}, \mathbb{M})$$

Assuming the sources are hyperon stars:

Formerly: GW + X-ray

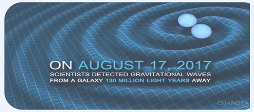

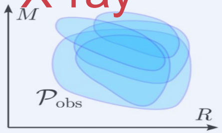

Presently: GW + X-ray + NUCL

$$\mathcal{L}_{\rm NUCL}(d_{\rm NUCL}|\boldsymbol{\theta}_{\rm EOS}) \propto \exp\left[-\frac{1}{2}\frac{(R_{\sigma\Lambda}-\bar{R}_{\sigma\Lambda})^2}{\sigma^2_{R_{\sigma\Lambda}}}\right]$$

$$\boldsymbol{\theta}_{\rm EOS} = \{R_{\sigma\Lambda}, R_{\omega\Lambda}\}$$

Strong linear $R_{\sigma\Lambda}$-$R_{\omega\Lambda}$ relations from fitting (with some statistical error) calculated Λ separation energies of **eleven** A ≥ 12 single Λ hypernuclei *(Rong, Tu & Zhou, 2021)*: $R_\omega = 1.228 R_\sigma - 0.097$

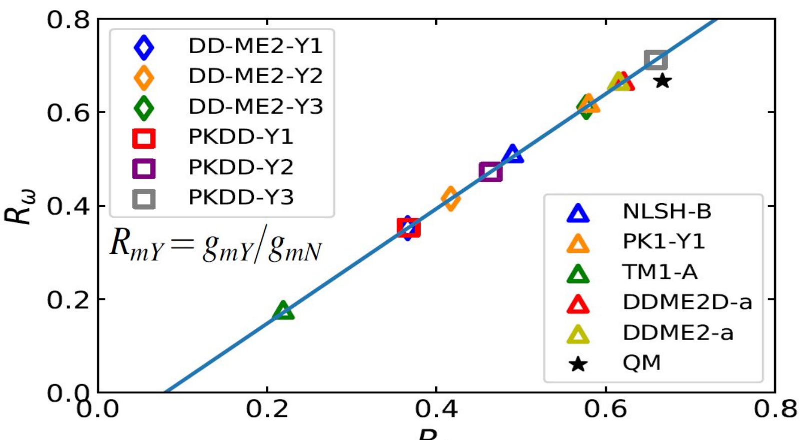

Hypernuclei	Exp.
$^{12}_{\Lambda}$C	11.36 ± 0.20
$^{13}_{\Lambda}$C	12.0 ± 0.2
$^{16}_{\Lambda}$O	13.0 ± 0.2
$^{28}_{\Lambda}$Si	17.2 ± 0.2
$^{32}_{\Lambda}$S	17.5 ± 0.5
$^{40}_{\Lambda}$Ca	18.7 ± 1.1
$^{51}_{\Lambda}$V	21.5 ± 0.6
$^{52}_{\Lambda}$V	21.8 ± 0.3
$^{89}_{\Lambda}$Y	23.6 ± 0.5
$^{139}_{\Lambda}$La	25.1 ± 1.2
$^{208}_{\Lambda}$Pb	26.9 ± 0.8

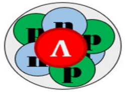

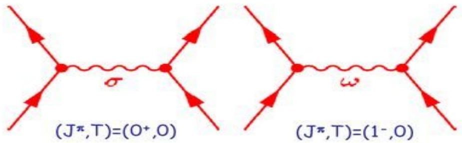

Linear $R_{\sigma\Lambda}$-$R_{\omega\Lambda}$ relations consistent with both finite-range meson-exchange and zero-range PC models

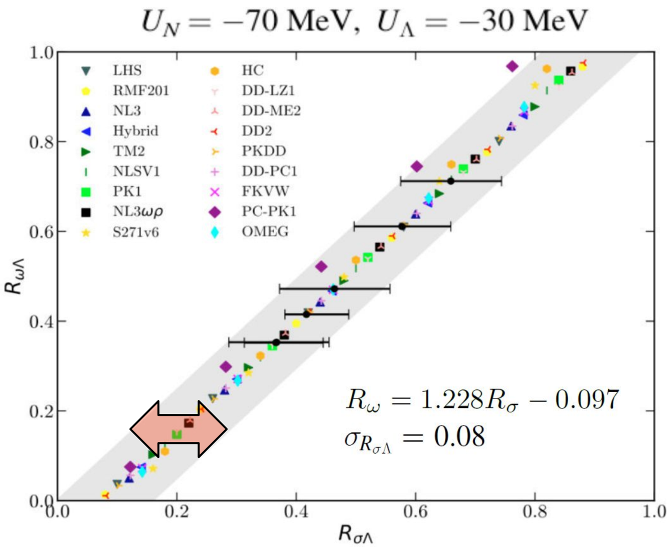

For finite-range interactions:

$$R_{\omega\Lambda} \approx \frac{-g_{\sigma N}\sigma}{U_N - g_{\sigma N}\sigma} R_{\sigma\Lambda} + \frac{U_\Lambda}{U_N - g_{\sigma N}\sigma}$$

For zero-range PC

$$R_{\omega\Lambda} \approx \frac{-\alpha_S^{NN}\rho_S}{U_N - \alpha_S^{NN}\rho_S - \beta_S^{NN}\rho_S^2 - \gamma_S^{NN}\rho_S^3 - \gamma_V^{NN}\rho_V^3} R_{\sigma\Lambda} + \frac{U_\Lambda}{U_N - \alpha_S^{NN}\rho_S - \beta_S^{NN}\rho_S^2 - \gamma_S^{NN}\rho_S^3 - \gamma_V^{NN}\rho_V^3}.$$

- Meson-exchange

$$\mathcal{L} = \mathcal{L}_{\rm free}^B + \mathcal{L}_{\rm int}^B + \mathcal{L}_m + \mathcal{L}_{\rm NL}$$

$$\mathcal{L}_{\rm free}^B = \sum_B \bar\psi_B[i\gamma_\mu\partial^\mu - m_B]\psi_B$$

$$\mathcal{L}_{\rm int}^B = \sum_B \bar\psi_B[-g_{\sigma B}\sigma - g_{\omega B}\gamma_\mu\omega^\mu - g_{\rho B}\gamma_\mu\vec\rho^\mu\cdot\vec\tau]\psi_B$$

$$\mathcal{L}_m = -\frac{1}{2}m_\sigma^2\sigma^2 + \frac{1}{2}m_\omega^2\omega_\mu\omega^\mu + \frac{1}{2}m_\rho^2\vec\rho_\mu\cdot\vec\rho^\mu + \frac{1}{2}\partial_\mu\sigma\partial^\mu\sigma - \frac{1}{4}\Omega_{\mu\nu}\Omega^{\mu\nu} - \frac{1}{4}\vec R_{\mu\nu}\cdot\vec R^{\mu\nu}$$

$$\mathcal{L}_{\rm NL} = -\frac{1}{3}g_2\sigma^3 - \frac{1}{4}g_3\sigma^4 + \frac{1}{4}c_3(\omega_\mu\omega^\mu)^2 + \Lambda_v(g_{\omega B}^2\omega_\mu\omega^\mu)(g_{\rho B}^2\rho_\mu\rho^\mu);$$

- Point-coupling

$$\mathcal{L}_{PC} = \mathcal{L}_{\rm free}^B + \mathcal{L}_{\rm 4f}^B + \mathcal{L}_{\rm hot}^B$$

$$\mathcal{L}_{\rm free}^B = \sum_B \bar\psi_B[i\gamma_\mu\partial^\mu - m_B]\psi_B$$

$$\mathcal{L}_{\rm 4f}^B = -\frac{1}{2}\Sigma_B\,\alpha_S^{NB}(\rho)(\bar\psi_N\psi_N)(\bar\psi_B\psi_B) - \frac{1}{2}\Sigma_B\,\alpha_V^{NB}(\rho)(\bar\psi_N\gamma_\nu\psi_N)(\bar\psi_B\gamma_\nu\psi_B) - \frac{1}{2}\Sigma_B\,\alpha_{TS}^{NB}(\rho)(\bar\psi_N\vec\tau\psi_N)(\bar\psi_B\vec\tau\psi_B) - \frac{1}{2}\Sigma_B\,\alpha_{TV}^{NB}(\rho)(\bar\psi_N\vec\tau\gamma_\nu\psi_N)(\bar\psi_B\vec\tau\gamma_\nu\psi_B)$$

$$\mathcal{L}_{\rm hot}^B = -\frac{1}{3}\beta_S^{NN}(\bar\psi_N\psi_N)^3 - \frac{1}{4}\gamma_S^{NN}(\bar\psi_N\psi_N)^4 - \frac{1}{4}\gamma_V^{NN}[(\bar\psi_N\gamma_\mu\psi_N)][(\bar\psi_N\gamma^\mu\psi_N)]^2,$$

#different statistical errors

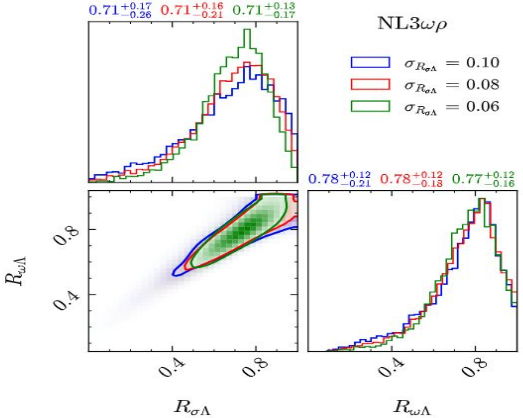

Hyperon star properties do NOT rely sensitively on the choice of the statistical error.

Adding relativistic Fock diagram: Similar correlation within statistical error

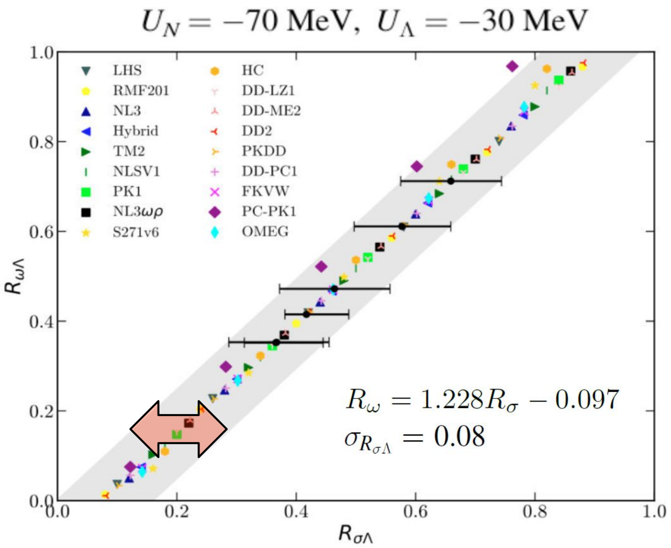

- Meson-exchange

$$\mathcal{L} = \mathcal{L}^B_{\text{free}} + \mathcal{L}^B_{\text{int}} + \mathcal{L}_m$$

- Point-coupling

$$\mathcal{L}_{PC} = \mathcal{L}^B_{\text{free}} + \mathcal{L}^B_{4\text{f}}$$

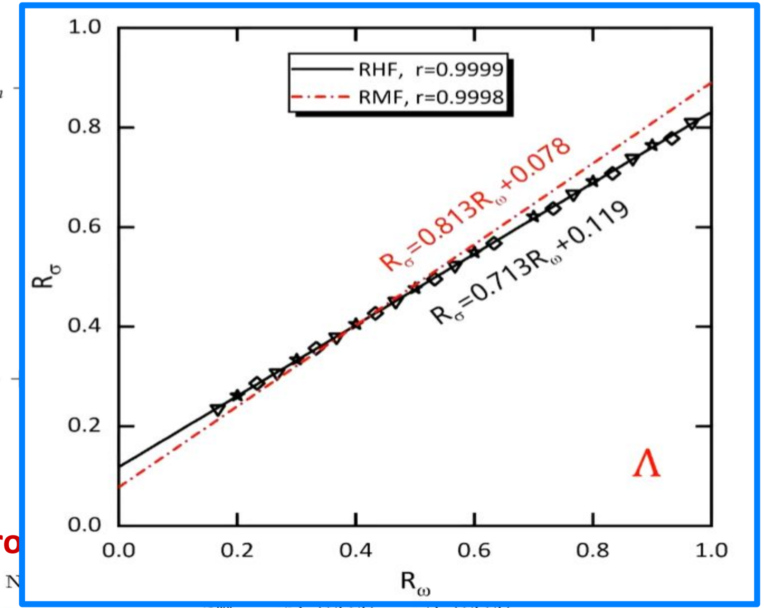

#different statistical erro

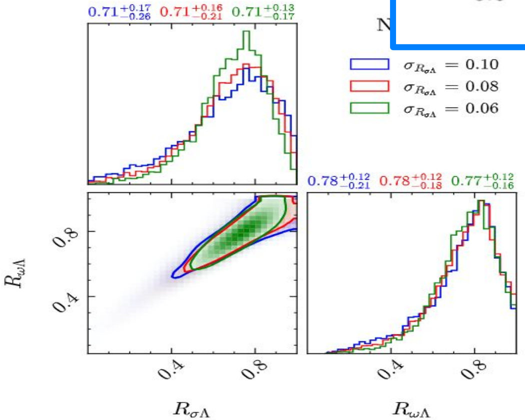

$$-\frac{1}{4}\gamma_V^{NN}[(\bar{\psi}_N\gamma_\mu\psi_N)][(\bar{\psi}_N\gamma^\mu\psi_N)]^2,$$

For finite-range interactions:

$$R_{\omega\Lambda} \approx \frac{-g_{\sigma N}\sigma}{U_N - g_{\sigma N}\sigma} R_{\sigma\Lambda} + \frac{U_\Lambda}{U_N - g_{\sigma N}\sigma}$$

For zero-range PC

$$R_{\omega\Lambda} \approx \frac{-\alpha_S^{NN}\rho_S}{U_N - \alpha_S^{NN}\rho_S - \beta_S^{NN}\rho_S^2 - \gamma_S^{NN}\rho_S^3 - \gamma_V^{NN}\rho_V^3} R_{\sigma\Lambda} + \frac{U_\Lambda}{U_N - \alpha_S^{NN}\rho_S - \beta_S^{NN}\rho_S^2 - \gamma_S^{NN}\rho_S^3 - \gamma_V^{NN}\rho_V^3}.$$

Hyperon star properties do NOT rely sensitively on the choice of the statistical error.

Bayesian inference of hyperon-nucleon interaction strengths from combining (binary) NS observations with hypernuclei experiments

- Finite size effects of the merging star alter late inspiral GW signal:

$$\mathcal{L}_{\mathrm{GW}}(d_{\mathrm{GW}}|\boldsymbol{\theta}_{\mathrm{GW}}, \mathbb{M}) \propto \exp\left[-2\int_0^\infty \frac{|\tilde{d}(f) - \tilde{h}(f, \boldsymbol{\theta}_{\mathrm{GW}})|^2}{S_n(f)} df\right],$$

$$\boldsymbol{\theta}_{\mathrm{GW}} = \{M_1, M_2, \Lambda_1, \Lambda_2, \chi_{1z}, \chi_{2z}, \varphi, \Psi, \theta_{\mathrm{jn}}, t_c, d_L, \mathrm{R.A.}, \mathrm{Decl.}\}$$

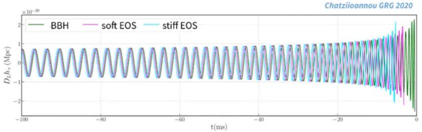

waveform depending on 17(4) parameters

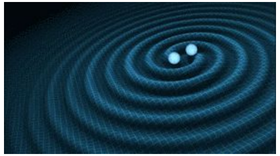

(1.36, 1.60) $M_\odot$
(1.16, 1.36) $M_\odot$

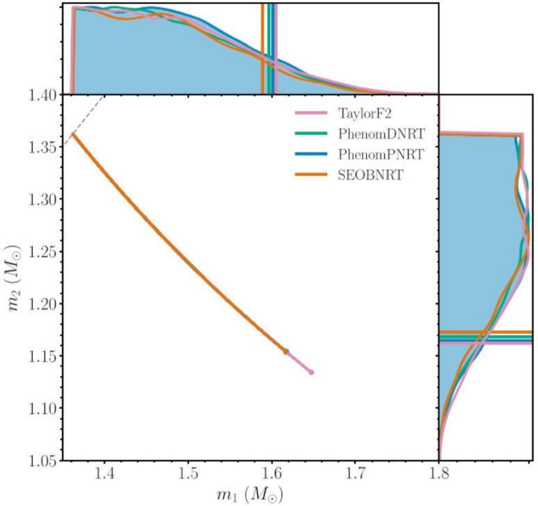

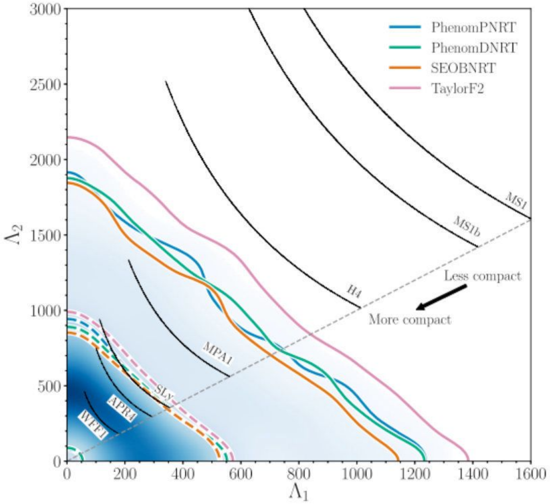

$$Q_{ij} = -\Lambda(EOS, m)m^5\varepsilon_{ij}$$

Bayesian inference of hyperon-nucleon interaction strengths from combining (binary) NS observations with hypernuclei experiments

- $\mathcal{L}_{\rm NICER}(M, R|\boldsymbol{\theta}_{\rm EOS} \cup \{\varepsilon_c\}, \mathbb{M}) = P_{\rm KDE}(M(\boldsymbol{\theta}_{\rm EOS}; \varepsilon_c), R(\boldsymbol{\theta}_{\rm EOS}; \varepsilon_c)),$

Kernel density estimation

Trace rays from hot spots on NS surface:

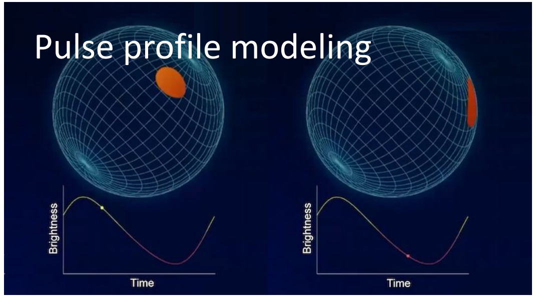

PSR J0030+0451

Miller et al, ApJL, 2019

$M = 1.44^{+0.15}_{-0.14} M_\odot \quad R = 13.02^{+1.24}_{-1.06}\,\text{km}$

Riley et al, ApJL, 2019

$M = 1.34^{+0.15}_{-0.16} M_\odot \quad R = 12.71^{+1.14}_{-1.19}\,\text{km}$

PSR J0740+6620

Miller et al, ApJL, 2021

$M = 2.062^{+0.090}_{-0.091} M_\odot \quad R = 13.71^{+2.61}_{-1.50}\,\text{km}$

Riley et al, ApJL, 2021

$M = 2.072^{+0.067}_{-0.066} M_\odot \quad R = 12.39^{+1.30}_{-0.98}\,\text{km}$

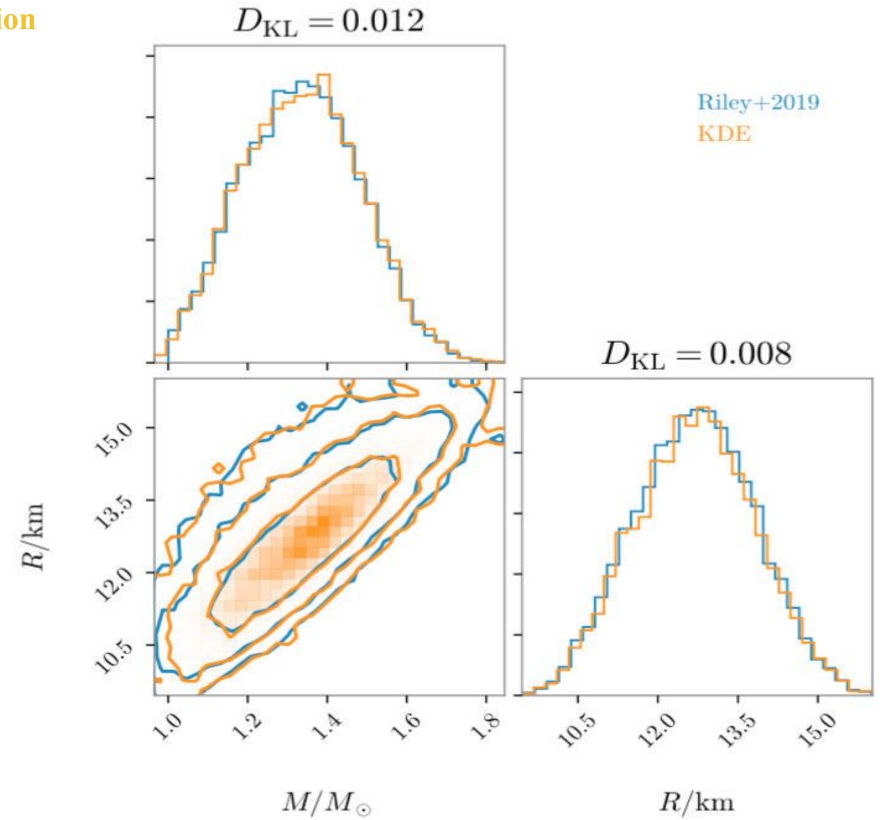

Bayesian inference of #hyperon-nucleon interaction strengths from combining (binary) NS observations with hypernuclei experiments

Likelihood

Posterior, Likelihood, Prior

$$p(\boldsymbol{\theta}|D, \mathbb{M}) = \frac{\mathcal{L}(D|\boldsymbol{\theta}, \mathbb{M})\pi(\boldsymbol{\theta})}{\int p(D|\boldsymbol{\theta}, \mathbb{M})\pi(\boldsymbol{\theta})d\boldsymbol{\theta}}$$

Parameter, Data, Model

- $$\mathcal{L}_{\rm NUCL}(d_{\rm NUCL}|\boldsymbol{\theta}_{\rm EOS}) \propto \exp\left[-\frac{1}{2}\frac{(R_{\sigma\Lambda} - \bar{R}_{\sigma\Lambda})^2}{\sigma^2_{R_{\sigma\Lambda}}}\right]$$
- $$\mathcal{L}_{\rm GW}(d_{\rm GW}|\boldsymbol{\theta}_{\rm GW}, \mathbb{M}) \propto \exp\left[-2\int_0^\infty \frac{|\tilde{d}(f) - \tilde{h}(f, \boldsymbol{\theta}_{\rm GW})|^2}{S_n(f)}df\right],$$
- $$\mathcal{L}_{\rm NICER}(M, R|\boldsymbol{\theta}_{\rm EOS} \cup \{\varepsilon_c\}, \mathbb{M}) = P_{\rm KDE}(M(\boldsymbol{\theta}_{\rm EOS}; \varepsilon_c), R(\boldsymbol{\theta}_{\rm EOS}; \varepsilon_c)),$$

new methodology

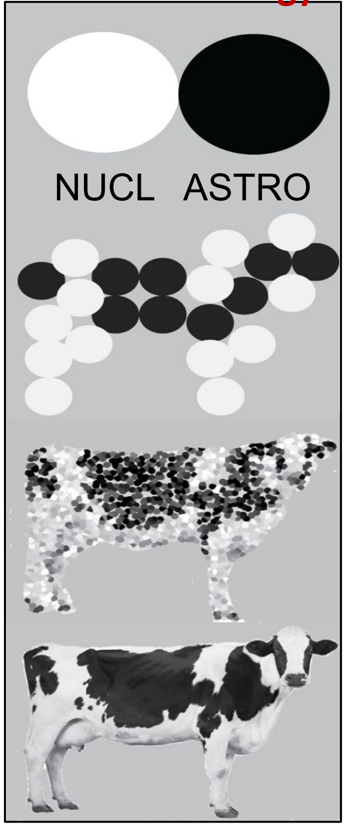

Software:
Bilby *(Ashton et al. 2019, version 0.5.5, https://git.ligo.org/lscsoft/bilby/),*
PyMultiNest *(Buchner 2016, version 2.6, https://github. com/JohannesBuchner/PyMultiNest),*
Toast *(Hernandez Vivanco et al. 2020, https://git.ligo.org/francisco.hernandez/toast),*
Corner *(Foreman-Mackey 2016, https://github.com/dfm/corner.py).*

Span uncertainty in YN interaction

#parameters and priors

$$\boldsymbol{\theta}_{\rm EOS} = \{R_{\sigma\Lambda}, R_{\omega\Lambda}\}$$

$$R_{\sigma\Lambda} \sim U[0,1]$$

$$\text{and } R_{\omega\Lambda} \sim U[0,1]$$

- ONLY explore the couplings of Λ hyperons;
- Keep Σ, Ξ hyperon couplings fixed to thei empirical values or based on SU(3) symmetry.

#posteriors

Most Probable Intervals of $R_{\sigma\Lambda}$ and $R_{\omega\Lambda}$ (68% Credible Intervals)

EOS	+NICER		+NICER +NUCL		+NICER +GW170817		+NICER +GW170817 +NUCL	
	$R_{\sigma\Lambda}$	$R_{\omega\Lambda}$	$R_{\sigma\Lambda}$	$R_{\omega\Lambda}$	$R_{\sigma\Lambda}$	$R_{\omega\Lambda}$	$R_{\sigma\Lambda}$	$R_{\omega\Lambda}$
LHS	$0.821^{+0.125}_{-0.463}$	$0.755^{+0.073}_{-0.155}$	$0.865^{+0.074}_{-0.208}$	$0.658^{+0.130}_{-0.194}$	$0.941^{+0.035}_{-0.048}$	$0.763^{+0.034}_{-0.028}$	$0.658^{+0.163}_{-0.251}$	$0.752^{+0.049}_{-0.095}$
RMF201	$0.760^{+0.186}_{-0.520}$	$0.759^{+0.081}_{-0.224}$	$0.658^{+0.172}_{-0.249}$	$0.672^{+0.138}_{-0.215}$	$0.949^{+0.032}_{-0.056}$	$0.769^{+0.035}_{-0.028}$	$0.842^{+0.090}_{-0.250}$	$0.754^{+0.061}_{-0.136}$
NL3	$0.424^{+0.330}_{-0.293}$	$0.746^{+0.156}_{-0.261}$	$0.681^{+0.171}_{-0.247}$	$0.768^{+0.136}_{-0.214}$	$0.399^{+0.379}_{-0.291}$	$0.794^{+0.128}_{-0.216}$	$0.765^{+0.130}_{-0.191}$	$0.840^{+0.101}_{-0.163}$
Hybrid	$0.363^{+0.381}_{-0.265}$	$0.807^{+0.132}_{-0.276}$	$0.750^{+0.130}_{-0.179}$	$0.865^{+0.096}_{-0.157}$	$0.305^{+0.388}_{-0.217}$	$0.764^{+0.143}_{-0.254}$	$0.777^{+0.118}_{-0.181}$	$0.869^{+0.090}_{-0.147}$
TM2	$0.311^{+0.330}_{-0.221}$	$0.751^{+0.179}_{-0.494}$	$0.736^{+0.145}_{-0.201}$	$0.856^{+0.102}_{-0.193}$	$0.323^{+0.487}_{-0.237}$	$0.784^{+0.158}_{-0.300}$	$0.772^{+0.137}_{-0.239}$	$0.870^{+0.086}_{-0.204}$
NLSV1	$0.252^{+0.285}_{-0.183}$	$0.756^{+0.167}_{-0.281}$	$0.688^{+0.117}_{-0.227}$	$0.863^{+0.100}_{-0.199}$	$0.247^{+0.279}_{-0.177}$	$0.744^{+0.182}_{-0.259}$	$0.689^{+0.122}_{-0.225}$	$0.866^{+0.100}_{-0.206}$
PK1	$0.254^{+0.273}_{-0.185}$	$0.756^{+0.172}_{-0.250}$	$0.687^{+0.139}_{-0.222}$	$0.869^{+0.099}_{-0.216}$	$0.248^{+0.271}_{-0.170}$	$0.754^{+0.176}_{-0.247}$	$0.683^{+0.130}_{-0.220}$	$0.867^{+0.101}_{-0.222}$
NL3$\omega\rho$	$0.384^{+0.393}_{-0.280}$	$0.773^{+0.147}_{-0.247}$	$0.690^{+0.163}_{-0.208}$	$0.759^{+0.131}_{-0.176}$	$0.420^{+0.448}_{-0.294}$	$0.777^{+0.127}_{-0.269}$	$0.712^{+0.157}_{-0.215}$	$0.778^{+0.121}_{-0.183}$
S271v6	$0.287^{+0.290}_{-0.207}$	$0.775^{+0.158}_{-0.232}$	$0.750^{+0.105}_{-0.144}$	$0.886^{+0.080}_{-0.128}$	$0.304^{+0.286}_{-0.083}$	$0.782^{+0.157}_{-0.230}$	$0.740^{+0.118}_{-0.161}$	$0.884^{+0.083}_{-0.147}$
HC	$0.266^{+0.253}_{-0.192}$	$0.517^{+0.316}_{-0.370}$	$0.733^{+0.110}_{-0.156}$	$0.902^{+0.070}_{-0.134}$	$0.266^{+0.304}_{-0.189}$	$0.783^{+0.157}_{-0.226}$	$0.737^{+0.106}_{-0.160}$	$0.902^{+0.072}_{-0.134}$
DD- LZ1	$0.298^{+0.321}_{-0.218}$	$0.775^{+0.152}_{-0.251}$	$0.769^{+0.122}_{-0.190}$	$0.871^{+0.083}_{-0.148}$	$0.327^{+0.381}_{-0.223}$	$0.792^{+0.142}_{-0.254}$	$0.772^{+0.128}_{-0.177}$	$0.870^{+0.087}_{-0.139}$
DD-ME2	$0.275^{+0.337}_{-0.192}$	$0.771^{+0.167}_{-0.299}$	$0.770^{+0.120}_{-0.172}$	$0.885^{+0.078}_{-0.137}$	$0.267^{+0.345}_{-0.188}$	$0.776^{+0.160}_{-0.237}$	$0.767^{+0.128}_{-0.168}$	$0.883^{+0.079}_{-0.124}$
DD2	$0.292^{+0.346}_{-0.205}$	$0.775^{+0.163}_{-0.252}$	$0.783^{+0.121}_{-0.173}$	$0.901^{+0.071}_{-0.135}$	$0.305^{+0.392}_{-0.221}$	$0.785^{+0.153}_{-0.276}$	$0.789^{+0.119}_{-0.157}$	$0.900^{+0.069}_{-0.120}$
PKDD	$0.267^{+0.347}_{-0.185}$	$0.806^{+0.140}_{-0.244}$	$0.820^{+0.095}_{-0.153}$	$0.930^{+0.051}_{-0.090}$	$0.282^{+0.420}_{-0.210}$	$0.813^{+0.136}_{-0.248}$	$0.835^{+0.102}_{-0.147}$	$0.932^{+0.047}_{-0.083}$
FKVW	$0.327^{+0.343}_{-0.236}$	$0.677^{+0.217}_{-0.260}$	$0.647^{+0.196}_{-0.250}$	$0.706^{+0.171}_{-0.211}$	$0.353^{+0.356}_{-0.240}$	$0.696^{+0.272}_{-0.203}$	$0.658^{+0.177}_{-0.254}$	$0.716^{+0.158}_{-0.217}$
PC-PK1	$0.283^{+0.310}_{-0.210}$	$0.701^{+0.215}_{-0.134}$	$0.650^{+0.150}_{-0.205}$	$0.770^{+0.147}_{-0.214}$	$0.282^{+0.319}_{-0.211}$	$0.703^{+0.212}_{-0.139}$	$0.651^{+0.148}_{-0.208}$	$0.771^{+0.146}_{-0.215}$
OMEG	$0.272^{+0.298}_{-0.194}$	$0.778^{+0.156}_{-0.244}$	$0.726^{+0.117}_{-0.171}$	$0.880^{+0.089}_{-0.153}$	$0.273^{+0.275}_{-0.188}$	$0.775^{+0.163}_{-0.242}$	$0.731^{+0.119}_{-0.167}$	$0.889^{+0.082}_{-0.152}$

Hyperon-nucleon interactions in the relativistic Lagrangian

- Hypernuclei constraint favors large values of $R_{\sigma\Lambda}$ and $R_{\omega\Lambda}$ and disfavors small values of both couplings;
- The addtion of astrophysical observational data on top of the laboratory $R_{\sigma\Lambda}$-$R_{\omega\Lambda}$ correlation rotates the linear correlation **slightly** towards the direction of small values of $R_{\omega\Lambda}$.

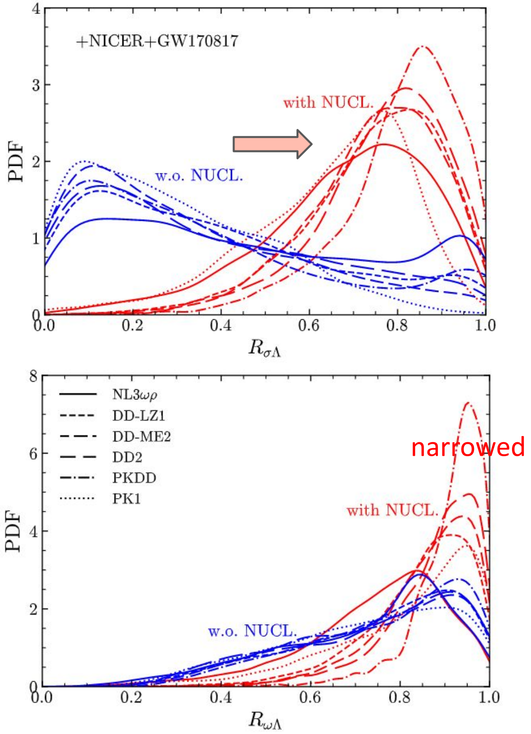

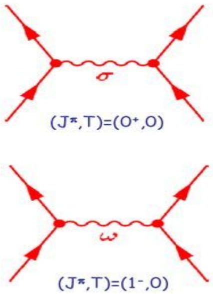

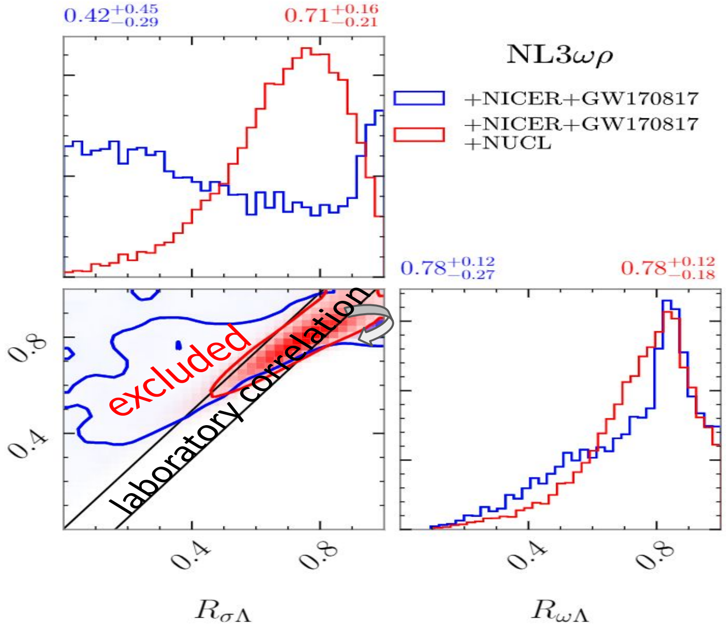

Hypernuclei results dominate !

Current status of the hypernuclear matter and hyperon star properties due to the uncertain YN+ interaction

- Taking the NL3ωρ one as an exemplary stiffest one;

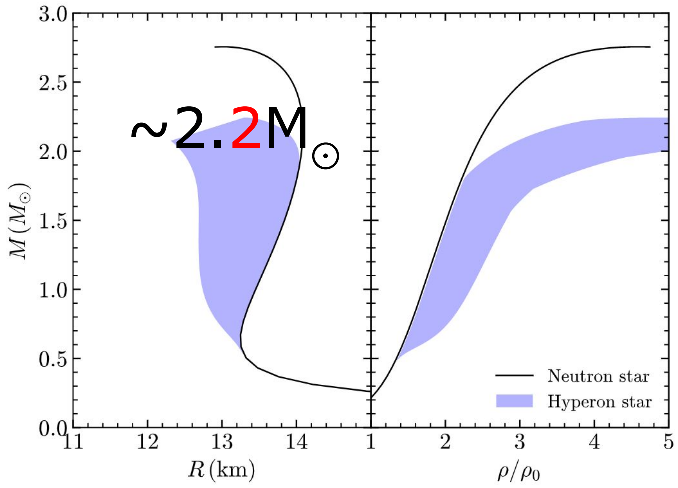

Due to hyperons, the maximum mass is **lowered by ~20%**: $M_{\max} = 2.176^{+0.085}_{-0.202}\, M_\odot$ 68% credible interval);

And the steller radius is smaller above ~0.5 $M_\odot$ and grows with the stellar mass.

2205.10631

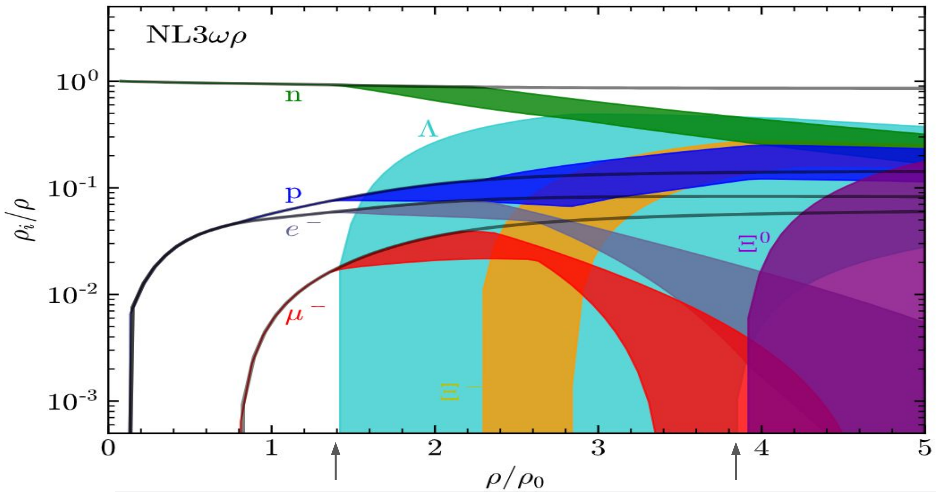

threshold density of Λ hyperons: 1.4-3.8ρ_0

Unclear whether Λ or Ξ− appear first.

In the following: +a few Ξ hypernuclei, ΛΛ hypernuclei

To include Ξ hypernuclei data

- Compared with Λ hypernuclei, Ξ hypernuclei are more difficult to produce and observe: Shorter lifetimes; Smaller cross sections;
- Fitting three s.p. separation energies of Ξ hypernuclei,

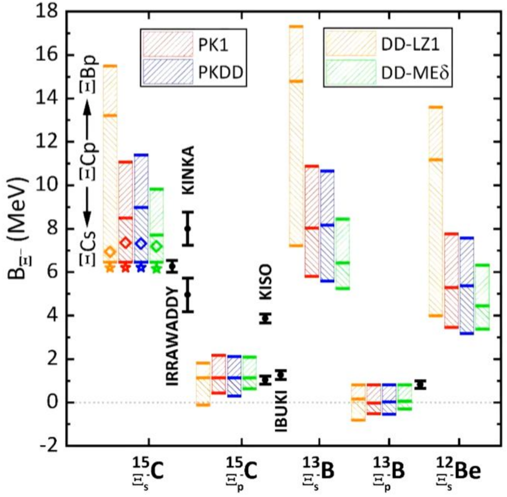

PRC 111 (2025) 014301

TABLE I. The ratio of σ-Ξ coupling strengths $g_{\sigma\Xi}/g_{\sigma N}$ for various RMF effective interactions, which are determined by fitting to the possible experimental values of the Ξ^- separation energy of $^{15}_{\Xi^-}$C in the 1s state [11] (denoted as ΞCs), in the 1p state [10] (denoted as ΞCp), and of $^{13}_{\Xi^-}$B in the 1p state [21] (denoted as ΞBp); see text for details. For other meson-hyperon coupling channels, the ratio of coupling strengthes are fixed to be $g_{\omega\Xi}/g_{\omega N} = 0.333$, $g_{\rho\Xi}/g_{\rho N} = 1.000$, $g_{\delta\Xi}/g_{\delta N} = 1.000$, and, additionally, the ω-Ξ tensor coupling $f_{\omega\Xi} = -0.400 g_{\omega\Xi}$.

	PK1	TW99	PKDD	DD-ME2	DD-MEX	DD-MEδ	DD-LZ1
ΞCs	0.304666	0.309145	0.312701	0.313264	0.309712	0.319533	0.305429
ΞCp	0.312236	0.318984	0.321078	0.322175	0.320552	0.324708	0.322607
ΞBp	0.320842	0.326105	0.328357	0.329127	0.326959	0.332777	0.327859

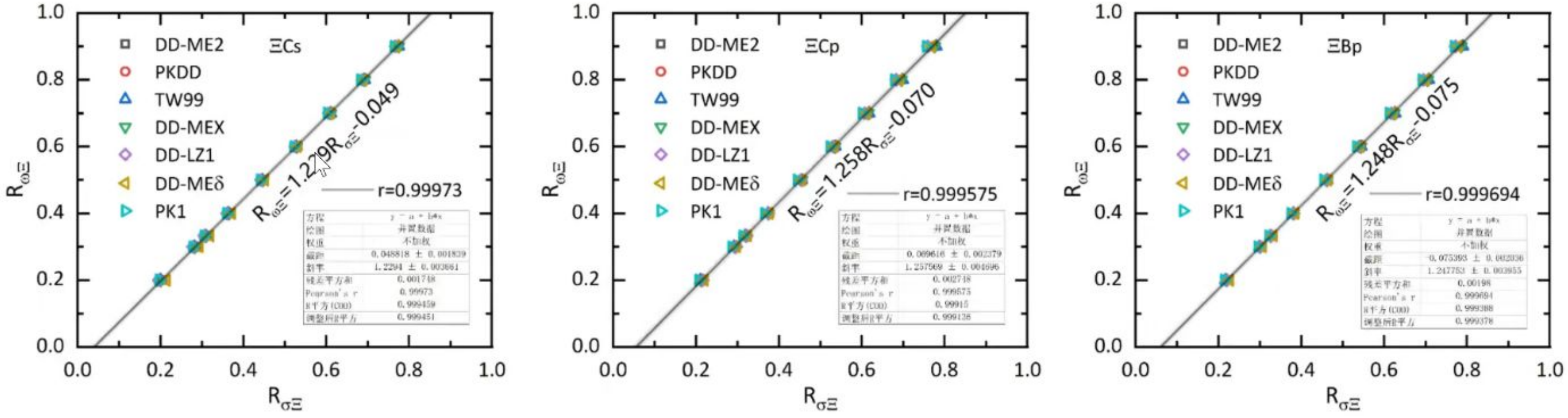

Adding likelyhood of Ξ hypernuclei

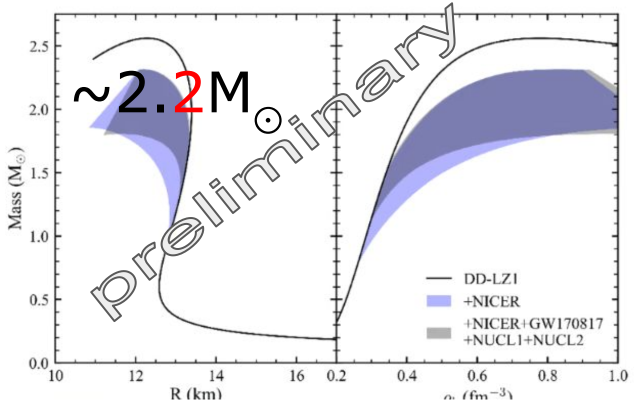

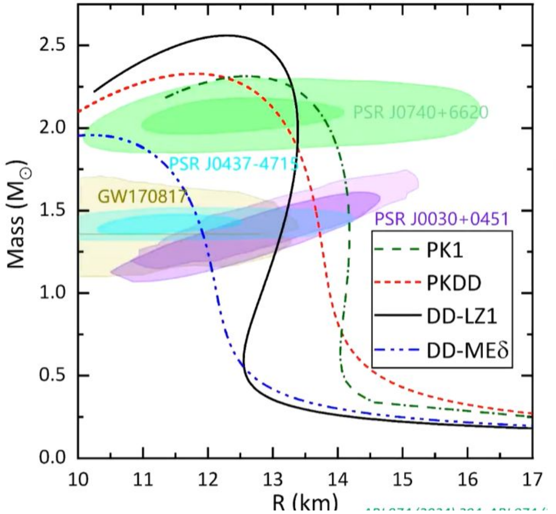

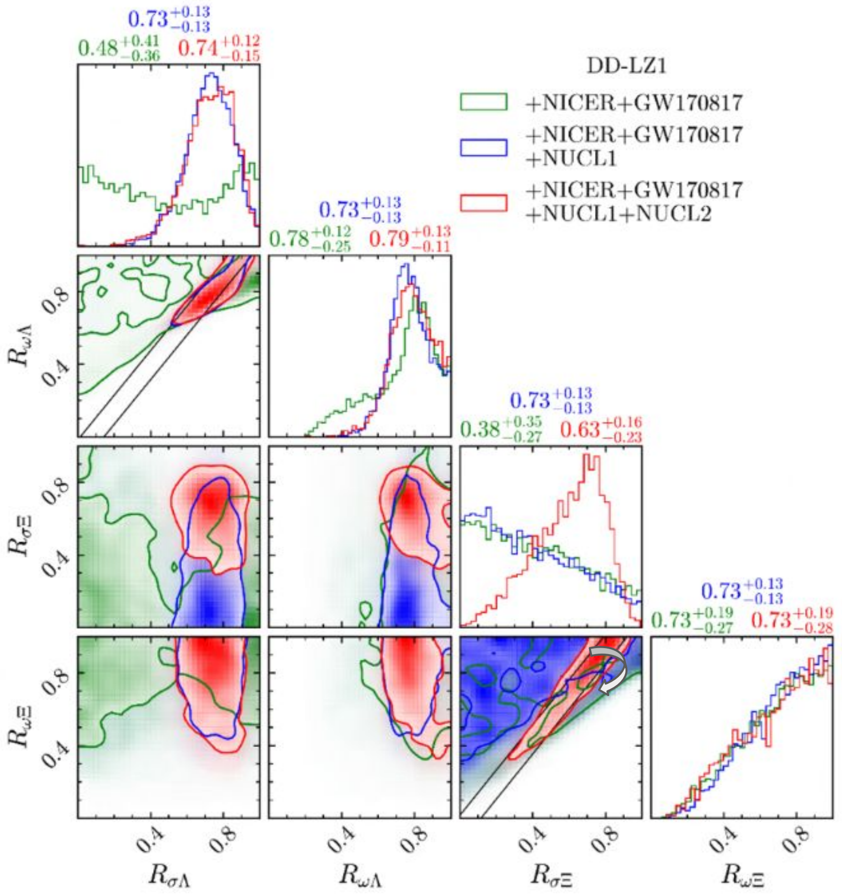

Short summary and Exciting future

- We incorporate new information from hypernuclei calculations to addresses a long-standing issue in NS physics;
- We find that the strong correlation between the scalar and vector channel of YN interactions indicated by s.p. separation energy of available Λ, Ξ hypernuclei ENSURE that there is **sufficient (vector) repulsion** and a prediction of hyperon stars with M_{max}~**2.2M**$_{\odot}$;
- Comprehensive analysis of multi-messenger, multi-wavelength data ongoing to probe the EoS at **different** density regimes ->

new methodology

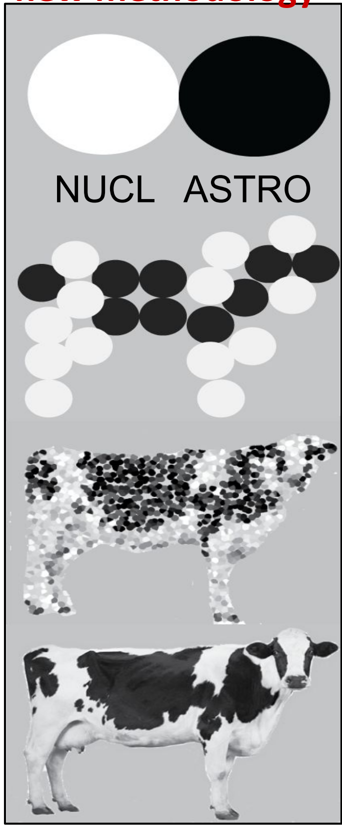

Connect consistently nuclear physics and GW+EM observations to probe the EoS at different density regimes (2021-)

Data:

GW event of GW170817(+GW190425) & **kilonova** light curve of AT2017gfo,

NICER×XMM-Newton's measurement of mass and radius of 2 PSRs,

(Mocked) **SKA**'s moment of inertia measurement on PSR J0737-3039,

Neutron-skin from PREX-II, CREX and the ab initio predictions on ^{208}Pb,^{40}Ca

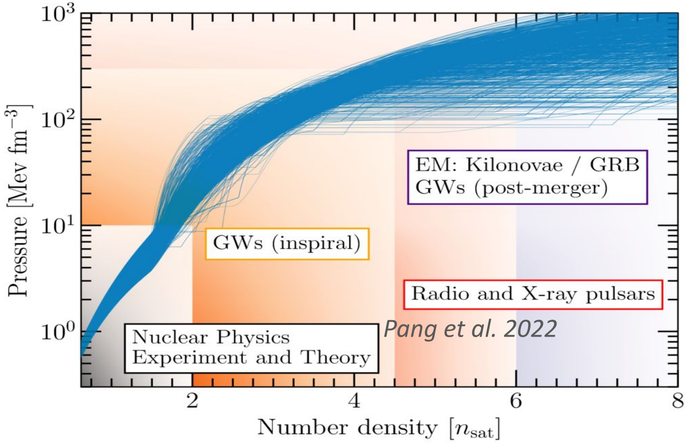

2021 | 2022 | 2023 | 2024

2021: Massive PSRs (radio)
+ GW (static tide)
+ X-ray (NICER) 2103.15119

2022: +mocked MOI (radio) 2107.07979
+DM 2204.05560

2023: +n skin 2305.16058
+hypernuclei 2205.10631
+kilonova (optical+) 2211.02007

2024: +GW (dynamic tide) 2305.08401
+X-ray (XMM-Newton) 2402.02799
+ΛΛ hypernuclei (in preparation)

Constraint on the pressure at densities ~1-3n_0 effectively tightened

PHYSICAL REVIEW D
covering particles, fields, gravitation, and cosmology

Highlights Recent Accepted Collections Authors Referees Search Press About

Thermal x-ray studies of neutron stars and the equation of state

Zhiqiang Miao, Liqiang Qi, Juan Zhang, Ang Li, and Mingyu Ge
Phys. Rev. D **109**, 123005 – Published 3 June 2024

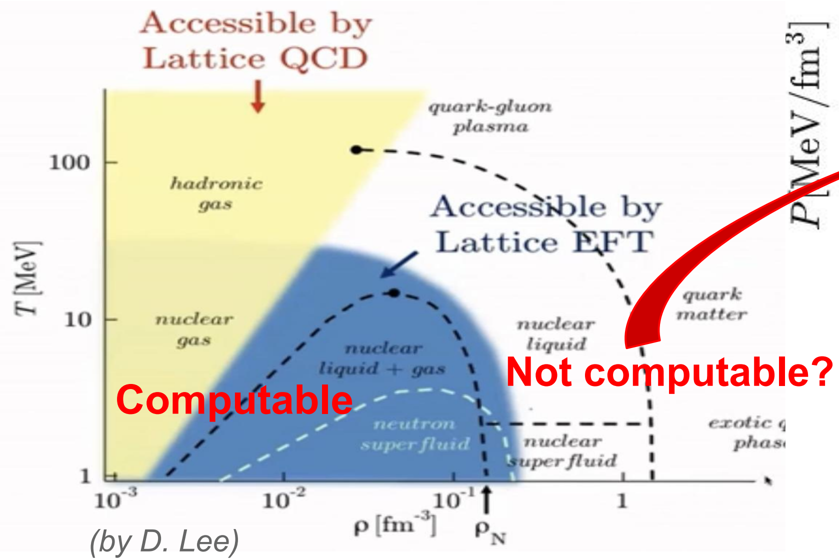

(by D. Lee)

2402.02799

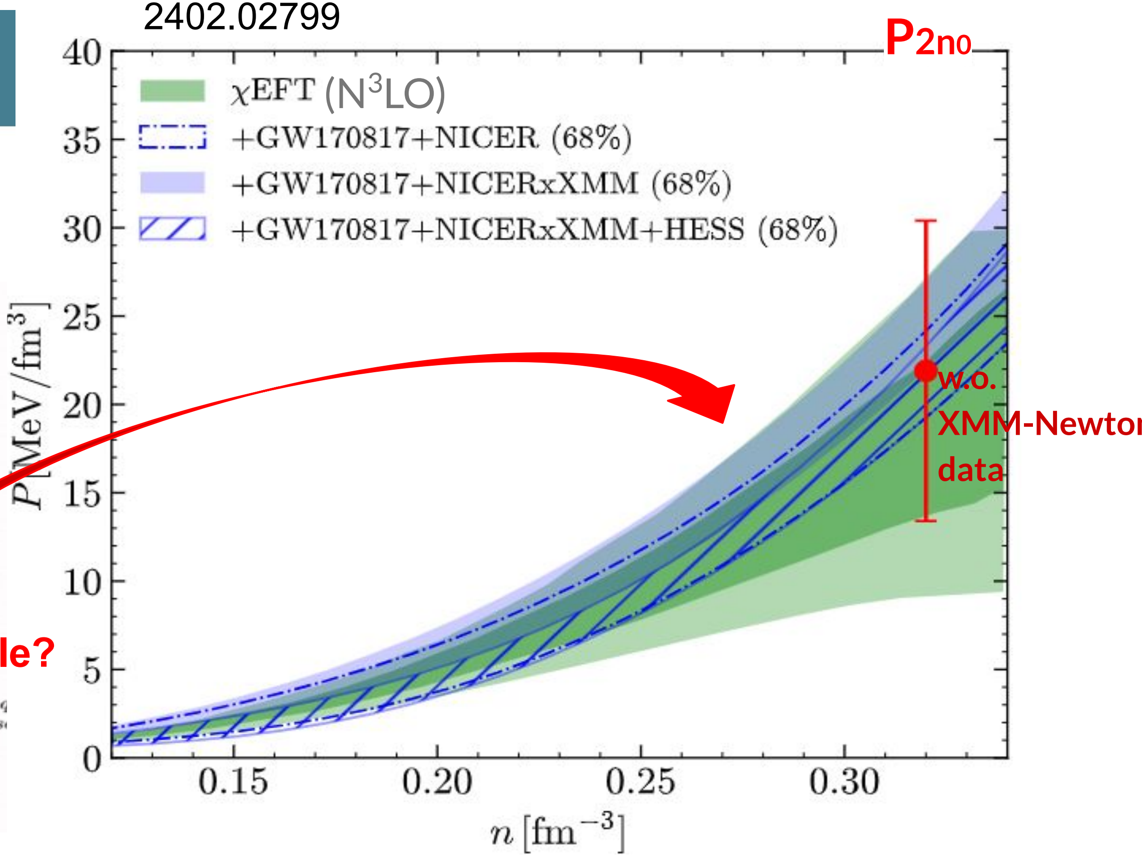

NICER view of PSR J0030+0451: MSP parameter estimation

Riley et al. 2019

Follow the propagation of light from the NS surface to the observer through the curved spacetime around the star;

Main difficulty lies in the degeneracy between **MANY** parameters it employs: (in addition to M, R) source D; H column density, parameters needed to describe the surface T map, angles encoding the orientation of this map with respect to the rotational axis and the observer's LOS;

Significant uncertainties in M,R estimate may be from **low counts** in the detected lightcurve or **noisy data** can lead to degeneracies between the model parameters or multi-modal posteriors:

XMM-Newton data can provide (indirect) NICER background constraint:
The introduction of the XMM-Newton data (EPIC MOS1 and MOS2) led to a reduction in background estimates from NICER-only data, resulting in higher compactness value:

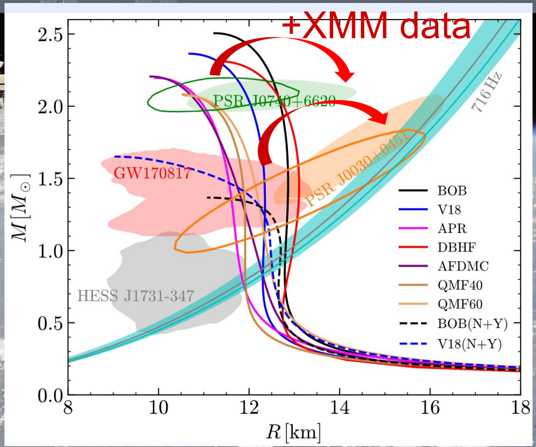

2402.02799

X-ray telescopes with **large effective area, high energy resolution, and high time resolution** in the soft X-ray band, as well as adequate imaging capability to discriminate the **background**:
<u>NICER</u> (2017), EP-FXT (2024), eXTP(~2030!), ATHENA(~2030).

"new precision era"

厦門大學天文學系

Department of Astronomy, Xiamen University

18 faculty members
11 postdocs
70 graduate students

Electromagnetic waves

Insight/ HXMT

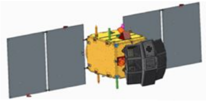

Einstein Probe (2024)

Radio | mm/sub-mm | FIR | MIR | NIR | V | NUV | UV | Soft X-ray | Hard X-ray | γ-ray

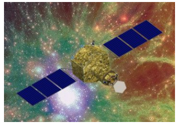

HUBS

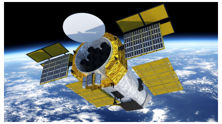

eXTP (~2030)

enhanced X-ray Timing and Polarimetry mission

Neutrinos

JUNO

Cosmic Rays

HERD

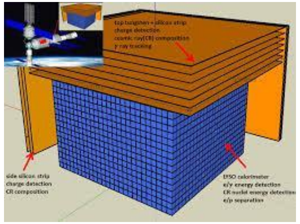

web: https://astro.xmu.edu.cn/

amen University

18 faculty members
11 postdocs
70 graduate students

gnetic waves


Insight/ HXMT

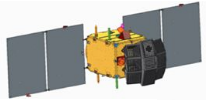
Einstein Probe (2024)

R | Soft X-ray | Hard X-ray | γ-ray

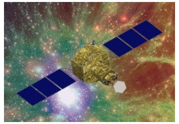
HUBS

Neut

JUNO

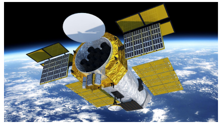
eXTP (~2030)

enhanced X-ray Timing and Polarimetry mission

web: https://astro.xmu.edu.cn/

What we learn so far

- ❑ Produce self-consistent framework for EoS modeling
- ❑ Check if constraints from all available constrains are fulfilled
  Demonstrate the consistency between laboratory and astrophysical nuclear matter in neutron stars by considering low-density nuclear physics constraints (from ^{208}Pb neutron-skin thickness) and high-density astrophysical constraints (from neutron star global properties).
- ❑ Prepare priors for a set of EoS parameters, also incorporating phase transitions
- ❑ Statistically establish the effective stiffness of neutron star EoS
  General requirements adopted (e.g., causality) indicate the EoS is moderately stiff, with sound speed squared peaked at $\sim 0.8c_s^2$ in NS matter, not subject to the type of phase transitions.
- ❑ Examine whether current data favour (strong) 1st-order phase transition inside NS cores
  Current data compatible with both possibilities; Evidence of a phase transition strengthened for stiff hadronic EoSs (like DD2); Perform preliminary test of the consistency of the parameters in the betastable NS matter and in the nearly symmetric nuclear matter formed in HIC
- ❑ **Confront Λ, Ξ hypernuclei data with the neutron star observational data**
  With the relaxation of the commonly-assumed SU(3) symmetry, the data of single Λ hypernuclei ensures a large enough scalar hyperon coupling to match the large vector hyperon coupling
- ❑ Suggest possibility to distinguish neutron stars with quark stars from simultaneous measurement of the stellar radius and the moment of inertia
  If the MOI is measured large for PSR J0737-3039 A, $I_A \gtrsim 1.4\times10^{45}$ g cm^2, it is most likely a quark star rather than a neutron star with or without a quark core, provided that the accuracy of the radius measurement is at least~1 km
- ❑ Comprehensive analysis of multi-messenger, multi-wavelength data ongoing to probe the EoS at different density regimes…

Thank you!